7-15-2016

Domains of STIP1 responsible for regulating PrPC-dependent amyloid-β oligomer toxicity.

Andrzej Maciejewski

Valeriy G Ostapchenko

Flavio H Beraldo

Vania F Prado

Marco A M Prado

See next page for additional authors

Authors
Andrzej Maciejewski, Valeriy G Ostapchenko, Flavio H Beraldo, Vania F Prado, Marco A M Prado, and Wing-Yiu Choy

Domains of STIP1 responsible for regulating the PrP^C-dependent amyloid-β oligomer toxicity

Andrzej Maciejewski*, Valeriy G. Ostapchenko†, Flavio H. Beraldo†, Vania F. Prado†, Marco A. M. Prado†[1], and Wing-Yiu Choy*[1]

*Department of Biochemistry, The University of Western Ontario, London, Ontario, Canada N6A 5C1

†Robarts Research Institute, Schulich School of Medicine & Dentistry, University of Western Ontario, London, Ontario, Canada, N6A5K8; Department of Anatomy and Cell Biology, Schulich School of Medicine & Dentistry, University of Western Ontario, London, Ontario, Canada, N6A5K8; Department of Physiology and Pharmacology, Schulich School of Medicine & Dentistry, University of Western Ontario, London, Ontario, Canada, N6A5K8

[1] To whom correspondence may be addressed (emails: jchoy4@uwo.ca; mprado@robarts.ca)

Short (page heading) title: TPR domains of STIP1 inhibit amyloid-β toxicity

ABSTRACT

Soluble oligomers of amyloid-beta (AβO) transmit neurotoxic signals through the cellular prion protein (PrP^C) in Alzheimer's disease (AD). Secreted stress-inducible phosphoprotein 1 (STIP1), an Hsp70 and Hsp90 cochaperone, inhibits AβO binding to PrP^C and protects neurons from AβO-induced cell death. Here, we investigated the molecular interactions between AβO and STIP1 binding to PrP^C and their effect on neuronal cell death. We showed that residues located in a short region of PrP (90-110) mediate AβO binding and we narrowed the major interaction in this site to amino acids 91-100. In contrast, multiple binding sites on STIP1 (DP1, TPR1 and TPR2A) contribute to PrP binding. DP1 bound the N-terminal of PrP (residues 23-95), while TPR1 and TPR2A showed binding to the C-terminal of PrP (residues 90-231). Importantly, only TPR1 and TPR2A directly inhibit both AβO binding to PrP and cell death. Furthermore, our structural studies reveal that TPR1 and TPR2A bind to PrP through distinct regions. The TPR2A interface was shown to be much more extensive and to partially overlap with the Hsp90 binding site. Our data show a possibility of a PrP, STIP1 and Hsp90 ternary complex, which may influence AβO-mediated cell death.

SUMMARY STATEMENT

This study reveals the molecular details of STIP1 and PrP binding regions upon complex formation and its implications in AβO toxicity in primary neuronal cell culture.

Keywords: Alzheimer's disease, neurotoxicity, neuroprotective, cochaperone, neuronal cell death

Abbreviations: AβO, soluble oligomers of the amyloid-beta peptide; AD, Alzheimer's disease; PrP^C, cellular prion protein; Hsp, Heat shock protein; HSQC, heteronuclear single quantum coherence; LTP, long-term potentiation; NMR, nuclear magnetic resonance; SPR, surface plasmon resonance; STIP1, stress-inducible phosphoprotein 1; TPR, tetratricopeptide repeat.

INTRODUCTION

Neurotoxic assemblies composed of soluble oligomers of the amyloid-beta peptide (AβO), derived from the sequential proteolytic cleavage of the amyloid precursor protein (APP), are thought to be critical for neurotoxicity in Alzheimer's disease (AD) [1, 2]. AβOs interact with numerous neuronal receptors or channel proteins resulting in impairment of synaptic plasticity, oxidative stress, disruption of Ca^{2+} homeostasis, inhibition of long-term potentiation (LTP) and neuronal cell death [3-6].

The cellular prion protein (PrP^C) is a high affinity AβO receptor that has garnered interest in relation to AβO-induced synaptic dysfunction [6-8]. PrP^C is a highly expressed cell surface glycoprotein which functions as a membrane scaffold for numerous ligands resulting in modulation of cellular signaling events [9]. PrP^C-AβO complex formation is coupled to activation of Fyn kinase through mGluR5 resulting in deregulation of NMDA receptors and calcium signaling [10-12]. Residues 23-27 and 95-110 of the disordered N-terminal region of PrP^C have been proposed to mediate AβO binding [6, 13, 14]. Moreover, impairment of binding to residues 95-110 seems to alleviate AβO neurotoxicity [6, 7]. While PrP^C is not essential for all AβO-induced deficits, inhibition of hippocampal LTP, impaired synaptic plasticity, loss of dendritic spines and neuronal cell death seem to be PrP^C-dependent [6, 8, 15]. Disruption of AβO binding by antibodies directed against PrP^C mitigate AβO induced neurotoxicity, suggesting that modulation of AβO-PrP^C interactions may be of therapeutic value in AD [7, 16-18]. Notably, a ligand of PrP^C, stress-inducible phosphoprotein 1 (STIP1), can inhibit AβO toxicity in neurons in a PrP^C-dependent manner [19]. Moreover, decreased levels of STIP1 in mammalian neurons or knockdown of STIP1 in *C. elegans* increases the toxicity of amyloid peptides [19, 20].

STIP1 is a cellular cochaperone that coordinates Hsp70 and Hsp90 interactions during folding of various cell cycle regulators and signal transduction proteins [21]. Interestingly, Hsp70, Hsp90 and STIP1 all can be secreted to the extracellular space through non-canonical pathways by extracellular vesicles, where they can increase cellular resilience by acting as extracellular chaperones or by signaling via membrane receptors [22-25]. In particular, STIP1 is secreted by astrocytes into the extracellular space, where it functions as a signaling molecule through PrP^C [22, 26]. Complex

formation with PrP^C induces neuroprotective and neuroproliferative signaling via PKA and ERK pathways, respectively [27, 28], which is initiated by Ca^{2+} influx through the α7 nicotinic acetylcholine receptor (α7nAChR) in hippocampal neurons [29].

STIP1 is a modular protein composed of three structurally related tetratricopeptide repeat domains (TPR1, TPR2A and TPR2B), as well as two aspartate-proline-rich regions (DP1 and DP2). Hsp engagement is facilitated through sequential interactions with the TPR domains. Binding of Hsp70 and Hsp90 to the TPR1/TPR2B and TPR2A domains of the cochaperone STI1P, respectively, allows the transfer of clients from Hsp70 to Hsp90 [21, 30-33]. However, recent work suggests that interaction between STIP1 and Hsp90 is comprised of more extensive interactions with the N-terminal domain and middle domain of Hsp90 [34, 35]. Previous work indicated that amino acids 113-128 within PrP^C are critical for STIP1 interaction [19, 26, 36]. Giving that STIP1 could potentially interact with PrP^C, Hsp90 and Hsp70 in the extracellular space, and this may modulate AβO toxicity, it is of importance to understand these protein interactions at the molecular level.

Here we provide structural insights into the roles of individual domains of STI1P in interacting with PrP as well as in inhibiting the AβO-PrP binding. In addition, the potential of complex formation between STI1P, PrP, and Hsp90 is explored. Our results reveal multiple domain interactions between STIP1 and PrP are involved in complex formation and that the Hsp-interacting domains, TPR1 and TPR2A, directly inhibit AβO binding to PrP and neuronal toxicity. In addition, we show that Hsp90 is able to influence the interaction of STIP1 with PrP, inhibiting the neuroprotective role of STIP1 against AβO insult.

MATERIALS AND METHODS

Protein expression and purification

pDEST17 expression vectors (Invitrogen) containing genes encoding various mouse STIP1 domains (i.e. full-length STIP1, TPR1 (residues 1 -118), DP1 (residues 119-216), TPR2A (residues 217-352), TPR2B (residues 353-480) and DP2 (residues 481-542)) with an additional N-terminal tobacco etch virus (TEV) cleavable 6xHis tag were transformed into *Escherichia coli* (*E. coli*) BL21 (DE3) pLysS strain. *E. coli* were grown in standard M9 minimal media at 37 ^{o}C to an OD_{600} of 0.9, at which point over-expression was induced with 1 mM isopropyl β-D-1-thiogalactopyranoside (IPTG). Temperature was reduced to 22 ^{o}C and cultures were grown overnight.

Proteins were initially purified by Ni^{2+}-affinity chromatography using Ni Sepharose 6 Fast Flow beads (GE Healthcare). 6xHis tag was cleaved by incubation with 6xHis tagged TEV overnight at room temperature. Following cleavage, TEV and 6xHis tag were removed by an additional Ni^{2+}-affinity chromatography purification [37]. For nuclear magnetic resonance (NMR) spectroscopy, protein was grown in standard M9 minimal medium supplemented with 1 g/L ^{15}N-labeled ammonium chloride. Proteins were flash-frozen in liquid nitrogen and stored at -80 ^{o}C for no longer than a month. All NMR studies were conducted with freshly prepared protein.

N-terminal 6xHis tagged recombinant mouse PrP (23-231), (90-231) and (23-95) in pRSETA was graciously provided by Dr. Kurt Wüthrich (ETH Zurich, Zurich, Switzerland). Plasmids were transformed into *E. coli* BL21 (DE3) and cultures were grown in lysogeny broth (LB) to an OD_{600} of 0.9. Expression was induced by the addition of 1 mM IPTG and cultures were grown overnight at 22 ^{o}C. Inclusion bodies were solubilized in 8 M urea containing 25 mM Tris, 500 mM NaCl, pH 7.5 and the resultant denatured protein was purified using Ni^{2+}-affinity chromatography. Solubilized protein was refolded by dialysis against 10 mM sodium acetate, pH 5. Purified protein was exchanged into 10 mM HEPES, pH 7, and the N-terminal 6xHis tag was cleaved by overnight incubation with thrombin (Haematologic Technologies Inc.). Thrombin was then removed by incubation with Benzamidine Sepharose 4 Fast Flow (GE Healthcare).

pET28 vectors encoding Hsp90β containing an N-terminal 6xHis tag separated by a thrombin cleavage site (kindly provided by Dr. Johannes Buchner) were purified as described in [35]. Plasmid

was transformed in *E. coli* BL21 (DE3) and cultures were grown in LB to an OD_{600} of 0.9 and induced with 1 mM IPTG. Temperature was dropped to 30 °C and cultures were grown overnight. Bacterial pellets were resuspended in 40 mM potassium phosphate, 400 mM KCl, 5 mM ATP, 1 mM $MgCl_2$, 6 mM imidazole, pH 8, and lyzed by French press at 10,000 psi. The resultant protein was purified using Ni^{2+} chromatography. Eluted fractions containing Hsp90β were combined and cleaved overnight by incubation with thrombin at 4 °C. Hsp90β was further purified by gel filtration chromatography with a Superdex S200 column equilibrated in 40 mM HEPES, 150 mM KCl, 5 mM $MgCl_2$, pH 7.5.

AβOs were prepared from $Aβ_{1-42}$ (rPeptide) as described previously [19]. Briefly, $Aβ_{1-42}$ was dissolved in 1,1,1,3,3,3-hexafluoro-2-propanol (HFIP) and SpeedVac centrifuged generating peptide films. $Aβ_{1-42}$ films were first re-suspended in DMSO to a concentration of 1 mM and diluted in PBS to a final working concentration of 100 μM or 150 μM for NMR experiments. Peptides were incubated for 24 hours at 4 °C and stored at -80 °C or used immediately.

NMR spectroscopy

Experiments were preformed on a Varian Inova 600 MHz NMR spectrometer equipped with xyz-gradient triple resonance probe at 25 °C in 5 mM sodium phosphate, pH 7. Data were processed with NMRPipe and analyzed using NMRView [38, 39]. Chemical shift changes were mapped onto PrP (90-231) structure based on a previously completed amide assignment (BMRB 16071 deposited in the BioMagResBank (http://www.bmrb.wisc.edu))[40]. Binding of preformed AβOs to PrP (90-231) and (23-95) was observed by ^{1}H-^{15}N HSQC spectra collected in the presence and absence of equimolar concentration (~85 μM) of AβO.

Backbone amide resonance assignments for TPR1 and TPR2A were obtained from the BioMagResBank under accession numbers 18691 and 18689, respectively [37]. ^{1}H-^{15}N HSQC spectra of ^{15}N-labelled TPR1 (50 μM) and TPR2A (50 μM) were collected in the absence and presence of PrP(23-231) (50 μM). The magnitude of chemical shift perturbations for traceable residues was calculated from the combined chemical shift changes in the ^{1}H and ^{15}N dimensions ($\Delta\omega$ (ppm) = $|0.2 * \Delta^{15}N| + |\Delta^{1}H^{N}|$) and mapped onto the crystal structures of TPR1 (PDB: 1ELW) and TPR2A (PDB:1ELR) [30].

Protein-protein binding assay

10 μg of full-length PrP or N-terminal PrP (23-95) were immobilized onto Falcon 96-well polystyrene plates by incubation overnight at 4 ^{o}C. Non-specific sites were blocked by incubation at room temperature for 1 hour with PBS-T (0.05%) containing 1% BSA. Plates were extensively washed with PBS-T and incubated with increasing concentrations of STIP1, different STIP1 domains, or Hsp90 for 1 hour. Following washing, bound proteins were detected using polyclonal antibodies directed towards STIP1 (1:10,000) in PBS-T. After subsequent washing, wells were probed with horseradish peroxidase (HRP)-conjugated anti-rabbit IgG (1:5000) (Bio-Rad) for 1 hour. The signal was visualized using o-phenylenediamine (OPD) and absorbance was measured at 495 nm by microplate reader.

For assessing PrP influence on Hsp90 binding to STIP1, polystyrene plates were covered with 10 μg of STIP1 and blocked as described above. After thorough washing, plates were incubated with various concentrations of PrP for 1 hour at room temperature, followed by incubation with 2 μM Hsp90 for 1 hour. After subsequent washing, wells were probed with rabbit anti-Hsp90 (1:1000, Cell Signaling) in PBS-T and bound Hsp90 was detected as outlined above.

TPR1 was labeled with Fluoroscein-5-Maleimide (Invitrogen) as per manufacturer's instructions to investigate competition of binding between TPR domains to PrP. PrP was adsorbed on to black polystyrene plates as described above. Plates were incubated with 1 μM fluorescein labeled TPR1 in the presence of various concentrations of TPR2A. Following washing, fluorescence was measured at excitation and emission wavelengths of 485/535 nm, respectively.

Surface plasmon resonance (SPR)

All SPR experiments were performed using a Biacore X system equipped with a CM 5 sensor chip (GE Healthcare). The chip was uniformly coated with PrP (23-231) using a standard amine-coupling method to an SPR signal of ~7000 resonance units (RU). Ligands were injected in 10 mM HEPES, 150 mM NaCl, pH 7, over an association period of 7 minutes at a flow rate of 5 μL/min. Off-kinetics were measured for an additional 2 minutes following the end of sample injections. The CM5 chip surface was regenerated using a 10 mM hydrochloric acid pulse for 1 minute at a flow rate of 100 μL/min between ligand injections.

Primary neuronal culture

Primary cultures of hippocampal neurons were obtained from E17.5 brains of wild-type ($Prnp^{+/+}$) mice from a C57BL6 background and prepared as previously described [19]. Hippocampi were aseptically dissected in HBSS (Invitrogen) and cells were dissociated in 0.25% trypsin at 37 ^{o}C for 20 minutes. Proteolysis was inactivated by re-suspension and dissociation of cells in Minimum Essential Media (MEM) (Invitrogen) supplemented with 10% Fetal Bovine Serum, penicillin (100 IU), streptomycin (100 μg/mL) and glucose (0.5%). Cultures were maintained on poly-lysine-coated coverslips or plates in Neurobasal Media (Invitrogen) supplemented with 2% B-27 (Invitrogen), penicillin (100 IU), streptomycin (100 μg/mL) and L-glutamine (500 μM). Half of the culture media was replaced every 3-4 days for the duration of the culture.

Cell death viability assay

Hippocampal cultures (10^5 cells/dish) were maintained for 11 days *in vitro* (DIV) then incubated with 1 μM AβO alone or in the presence of STIP1 (1 μM), TPR1 (2 μM), TPR2A (2 μM) or DP1 (2 μM) for 48 hours. Cell death was assayed using LIVE/DEAD Viability/Cytotoxicity Kit for mammalian cells (Invitrogen) as described by the manufacturer. NIH ImageJ Cell Counter plug-in was used to calculate percentage of dead cells (number of dead cells / (number of dead cells + number of viable cells)). For Hsp90 and AβO co-incubation experiments, cell cultures were incubated in the presence or absence of Hsp90 (2 μM) and AβO (1 μM) with various concentrations of STIP1 (0-600 nM) and incubated for 48 hours. Cell death was assayed as described above.

AβO binding to primary hippocampal neurons

13 DIV cultured neurons (6 x 10^4 cells/dish) were treated for 15 minutes with 200 nM AβO alone or in the presence of 500 nM STIP1 or 1 μM TPR1, TPR2A and DP1 at 37 ^{o}C. Following incubation, cells were washed with KRH buffer (125 mM NaCl, 5mM KCl, 1.8 mM $CaCl_2$, 2.6 mM $MgSO_4$, 10 mM glucose, 5 mM HEPES, pH 7.2). Cells were fixed with 4% paraformaldehyde for 20 minutes, washed with PBS, permeabilized with 0.5% Triton X-100 in PBS for 5 minutes and blocked with 5% BSA (Sigma-Aldrich) in PBS for 1 hour at room temperature. Coverslips were incubated with antibodies against γ-tubulin (1:500; Abcam) and amyloid-β (6E10, 1:350; Covance) overnight at 4 ^{o}C.

γ-tubulin and amyloid-β were detected by subsequent incubation with secondary Alexa Fluor-488 and Alexa Fluor-633-conjugated antibodies (Invitrogen), respectively, for 1 hour at room temperature. Immunofluorescence was detected on an LSM510 confocal microscope equipped with a 63x/1.4NA oil-immersion objective lens. The resultant fluorescence from neurites was integrated using NIH ImageJ software.

RESULTS

Mapping of AβO interface on PrP

Previous studies have revealed that residues 95-110 of PrP^C play a pivotal role in mediating the interaction with AβO [6, 13, 16]. To refine the AβO binding-site on PrP in a residue specific basis, we performed ^1H-^{15}N-HSQC experiments on ^{15}N-labelled PrP (90-231) in the absence and presence of preformed AβO at a 1:1 molar ratio (Figure 1A). A significant decrease in signal intensity was observed for amide resonances spanning residues 90-110 of the disordered N-terminal of PrP (Figure 1C), while no new NMR peaks were observed in the PrP spectrum upon the addition of AβO. This loss in signal intensity is likely due to peak broadening resultant from residues 90-110 binding a large molecular weight species of AβO. No significant systematic changes in intensity were observed for C-terminal resonances, suggesting the AβO binding site is highly localized to the region spanning residues 90-110 of PrP (90-231) (Figures 1B and 1C). The greatest decreases in peak intensity were observed in a glycine-rich region N-terminal of the sequence (residues 91-100). Interestingly, small but notable chemical shifts were observed for C-terminal residues Leu125, His140, Gly142, Asn174 Val180, Asn181, His187, Thr188 and Val189. These changes are likely due to weak transient interactions with AβO or moderate conformational changes in PrP upon AβO binding. Unfortunately, we were unable to assign the N-terminal of PrP, residues 23-95, due to the high sequence redundancy and signal overlap of the spectrum. However, no significant intensity changes or chemical shift perturbations were seen in the visible peaks of the disordered N-terminal fragment PrP (23-95) in the presence of AβO (Figure 1D), which stresses the importance of residues 90-110 in PrP-AβO complex formation.

Identification of STIP1 binding domains of PrP

We next sought to identify domains of STIP1 that bind PrP and the respective regions of PrP that mediate the interactions. Previous studies have identified the TPR2A domain of STIP1 as the major interaction site for PrP [19, 26, 36]. However, additional regions of STIP1 may be involved in PrP binding due to the modular structure of STIP1 and the structural similarity shared between its TPR domains. Of particular interest were STIP1 domains that specifically bind to PrP (90-231), since they may impair PrP-AβO complex and provide a mechanistic basis for STIP1 neuroprotective properties against AβO insult [19]. We tested binding of STIP1 and its domains using a multi-well protein-

binding assay. The domain boundaries of STIP1 are shown in Figure 2A. We confirmed that STIP1 specifically bound PrP with high affinity (Figure 2B, K_d = 186±15 nM), which is in agreement with previous studies [26]. Probing full-length PrP with individual domains of STIP1 revealed that TPR1 (K_d = 1.2±0.2 μM) and DP1 (K_d = 600±50 nM), in addition to the previously reported TPR2A (K_d = 800±130 nM) domain, can also interact with PrP with comparable affinity, albeit lower than the affinity of full length STIP1 (Figure 2C). The DP1 domain of STIP1 was capable of interacting in a specific and saturable manner with an N-terminal fragment of PrP (23-95), whereas the other domains (TPR1 and TPR2A) did not (Figure 2D). The results strongly suggest that DP1 interacts with the disordered N-terminal fragment of PrP (23-95), while PrP (90-231) binds TPR1 and TPR2A. The result is consistent with finding of previous studies showing that residues 113-128 of mouse PrP is responsible for mediating the interaction with the TPR2A domain of STI1P [26].

Since TPR1 and TPR2A both bind the C-terminal fragment of PrP (90-231), we investigated whether these domains can bind simultaneously or compete for binding to PrP. TPR2A was capable of displacing fluorescently labeled TPR1 from its complex with PrP in a concentration-dependent manner suggesting that binding of TPR1 and TPR2A to PrP is mutually exclusive (i.e. the TPR1 and TPR2A binding sites on PrP are either overlapping or in close proximity) (Figure 2E).

TPR1 and TPR2A prevent AβO binding to PrP

We have previously demonstrated that the TPR2A domain of STIP1 is able to inhibit AβO binding to PrP, albeit with lower potency than full length STIP1 [19]. Given that TPR1 and TPR2A can both bind to the C-terminal part of PrP (residues 90-231), we investigated whether TPR1 can modulate AβO-PrP binding by surface plasmon resonance (SPR). AβO injections showed a dose-dependent increase in response monitored by SPR indicating binding (Figure 3A). Co-injection of STIP1 (62.5 nM) with a constant concentration of AβO showed an appreciable decrease in the response signal, suggesting inhibition of AβO binding to PrP. When co-injected with 125 nM STIP1, the response from AβO was equal to that of an injection of 125 nM STIP1 alone, suggesting complete inhibition of AβO binding (Figure 3B). Injections of TPR1 or TPR2A domains also inhibited AβO binding to PrP in a dose-dependent manner, albeit at higher concentrations than full-length STIP1 (Figures 3C and 3D, respectively). DP1, which binds the N-terminal region of PrP (residues 23-95), did not have any effect on AβO signals, consistent with this region being dispensable for AβO binding to PrP (Figure 3E).

Injection of each domain individually produced no detectable signal likely due to their small size and sensitivity of the instrument (data not shown). These results suggest that both the TPR1 and the TPR2A domains of STIP1 contribute to the direct inhibition of AβO binding to PrP through interactions with PrP (90-231).

TPR1 and TPR2A inhibit AβO binding and toxicity in neurons

STIP1 is a neuroprotective regulator of AβO toxicity in hippocampal neurons and TPR2A domain by itself can reproduce this effect [19]. We therefore investigated whether *in vitro* inhibition of AβO binding to PrP by TPR1 can also translate to a beneficiary response in cultured primary mouse hippocampal neurons. Ectopic treatment of neurons with recombinant STIP1, TPR1 or TPR2A domains in the presence of AβO significantly decreased AβO binding to neuronal cell bodies compared to treatment with AβO alone (Figures 4A and 4B). Co-treatment of neuronal cultures with AβO and DP1 resulted in no visible effect on the amount of AβO bound to neurites. These observations reflected our *in vitro* SPR results where only the TPR1 and TPR2A domains, but not DP1, were able to inhibit AβO binding to PrP in a concentration-dependent manor. To assess if the decrease in AβO binding translated to inhibition of AβO cytotoxicity, primary hippocampal neurons were treated with AβO in the presence or absence of STIP1, TPR1, TPR2A or DP1 and incubated for 48 hours before assessing the number of dead cells. AβO treatment alone increased cell death by ~15% compared to basal levels. Co-treatment with STIP1, TPR1 or TPR2A rescued neuronal death from AβO induced toxicity (Figure 4C). No discernible effect on cell viability was seen in cells co-treated with DP1 and AβO compared to AβO treatment alone.

Mapping of TPR1 and TPR2A interfaces mediating PrP binding

To gain molecular understanding of the STIP1-PrP interactions, NMR spectroscopy was used to map the binding interfaces of PrP on TPR1 and TPR2A on a residue-specific manner. $^{1}H^{-15}N$ HSQC spectra of TPR1 and TPR2A showed comparable amplitude of chemical shift perturbations upon addition of PrP (Figures 5A and 5C). Resonances undergoing fast exchange (i.e. chemical shift difference between the free and bound states is small compared to the rate of exchange between these two states) were traced upon titration of PrP and were mapped onto the crystal structures of TPR1 and TPR2A (Figures 5B and 5D). Notable chemical shift changes were observed for residues Asp70,

Trp71, Gly98, Lys100, His101 and Ala103 of TPR1, which form a contiguous patch on the surface of the C-terminal part of the TPR1 structure (Figure 5B). In contrast, the TPR2A binding interface for PrP is more extensive, extending diagonally across a hydrophobic cradle-shaped groove on one side of the TPR2A molecule. Interestingly, this cradle-shaped groove is reserved for binding of the C-terminal peptide of Hsp90 to fulfill STIP1 cochaperone function during protein client folding [30]. While critical contacts between TPR2A and Hsp90 C-terminal peptide made by the carboxylate clamp (Lys229, Asn233, Asn264, Lys301, Arg305) of TPR2A did not show the largest chemical shift changes upon binding of PrP, the partial overlap between the Hsp90 and PrP binding interfaces suggests that Hsp90 and PrP may regulate each other's binding to STIP1 (Figure 6A). Therefore, we examined the potential for cooperative binding and complex formation for STIP1, PrP and Hsp90.

STIP1 was adsorbed onto polystyrene plates and probed with PrP. Following thorough washing of the complex; plates were incubated with a constant amount of Hsp90 (4 μM) and bound Hsp90 was detected using antibodies directed against Hsp90. Intriguingly, by increasing the concentration of PrP we achieved a saturable increase in Hsp90 binding to the plate (Figure 6B). In contrast, no Hsp90 binding was detected to PrP immobilized onto a polystyrene plate in the absence of STIP1 (Figure 6C). These data suggest that PrP binding to STIP1 may induce conformational changes in the complex, which in turn may increase the recruitment of Hsp90.

To investigate the potential relevance for the ternary complex formation of STIP1, Hsp90 and PrP in AβO toxicity, primary mouse hippocampal neurons were incubated in the presence of AβO (1 μM) and sub-optimal concentrations of STIP1. STIP1 caused a dose-dependent decrease of AβO-induced cell death (Figure 6D). However, addition of excess recombinant Hsp90 (2 μM) prevented STIP1 neuroprotection against AβO (Figure 6D). These results suggest that excess Hsp90 is able to block STIP1 neuroprotective signaling, potentially by sequestering the protein or by interfering with signaling events through PrP at the cellular membrane.

DISCUSSION

AβOs have been demonstrated to trigger synaptic dysfunction through interactions with several neuronal receptors [3-5, 41]. Numerous studies have identified PrP^C as a high affinity receptor for AβOs and implicated the interaction in the transmission of neurotoxic signaling [6, 15, 17]. Disruption of the PrP^C-AβO complex has shown therapeutic merit in the reduction of AβO toxicity [7, 19]. We have recently determined that the cellular cochaperone and physiological PrP^C ligand STIP1 is able to directly inhibit AβO binding to PrP^C and alleviate synaptic loss, depression of long-term potentiation and neuronal cell death [19]. Therefore, understanding how this complex is modulated is of importance.

The studies reported here provide molecular insights regarding the functional modules of STIP1 that directly contribute to its recently described protective role against AβO neurotoxicity and structural details of regions involved in binding to PrP. Our NMR studies revealed significant resonance attenuations in the N-terminal unstructured region of PrP encompassing residues 90-110 upon binding of mature preformed AβOs, suggesting these residues mediate complex formation. These results are consistent with previous observations, which indicated residues centered around 95-110 are essential and sufficient for AβO binding to PrP [6, 7, 13, 14]. No significant chemical shift changes were observed upon the addition of AβO to N-terminal PrP (23-95). A short highly basic charge cluster 'KKRPK' located in the far N-terminal of PrP (residues 23-27) has been suggested as a secondary AβO binding; however, other groups have reported near identical AβO binding levels to PrP (90-231) as wild-type PrP [13, 42]. It is possible the charge cluster acts as a secondary binding event following initial association of AβO to the primary binding site (residues 90-110). Thus, residues 23-95 may not participate in binding in the absence of the high affinity site, which could explain the lack of large chemical shift perturbations of PrP (23-95). Unfortunately, due to high sequence redundancy and peak overlap problems owning to its disordered properties, we were unable to assign residues 23-95 of PrP constructs. Thus, we cannot rule out the possibility of minor, but localized chemical shift changes in residues 23-95 upon AβO titration.

Small chemical shift changes were noted for C-terminal PrP residues mapping to α-helices 1 and 2. These changes were much smaller in magnitude than those observed for the primary AβO

binding site. These findings are unexpected, since the globular part of C-terminal portion of PrP is thought to be dispensable in its interaction with AβO. These changes may result from conformational alterations in helix 1-helix 2 of PrP upon AβO interaction. Alternatively, transient contacts between PrP molecules may be induced upon binding to Aβ aggregates, stabilizing these complexes. Indeed, competition experiments targeting an epitope spanning residues 131-153 effectively disrupted AβO binding to PrP [7].

Our protein-protein binding assay results showed that full-length STIP1 binds to PrP (23-231) with high affinity (K_d ~186 nM), which is in agreement with previous finding [26, 36]. Surprisingly, binding of different domains of STIP1 to PrP (23-231) indicated that not only previously identified TPR2A, but also the structurally related TPR1 domain and the DP1 domain bind PrP with high affinity. TPR2A was capable of displacing TPR1 binding to PrP suggesting that they have overlapping binding sites or TPR2A is capable of occluding the TPR1 binding site on PrP. Interestingly, DP1 domain bound to the N-terminal of PrP (residues 23-95), while the TPR domains did not, suggesting their binding-site on PrP lies within residues 90-231. The recently solved NMR structures of the DP1 and DP2 domains of yeast STIP1 reveal a novel α-helical fold composed of 6 and 5 helices, respectively [35]. Electrostatic potentials of DP1 illustrate a slightly positive groove containing an additional α-helix absent in DP2, which stabilizes secondary structure elements in DP1. Consequently, while both DP1 and DP2 share a common tertiary structure, these distinct structural differences may indicate the inability of DP2 to bind to the N-terminal of PrP.

Even though the function of the DP domains remains uncertain, the length of the linker between TPR1 and TPR2A, which includes the DP1 domain, has recently been proposed to facilitate transfer of Hsp90 from TPR1 to TPR2B during protein client folding [33]. This is the first study to identify a direct ligand of DP1, suggesting the domain may influence STIP1 binding to physiological ligands outside of its cochaperone role in client protein refolding.

We confirmed by SPR the dose-dependent specific interaction between immobilized PrP and AβO. Due to the abnormally long dissociation kinetics, consistent with other studies, we were unable to quantitatively determine a binding constant for the interaction [13, 19, 43]. Thus, the effects of STIP1 and individual domains on AβO were assessed qualitatively based on the absolute magnitude of the

response change. STIP1 effectively inhibited AβO binding to PrP, abolishing the interaction at low nanomolar concentrations, as demonstrated previously [19]. TPR2A and TPR1 domains were also capable of inhibiting AβO binding to PrP albeit at much greater concentrations than STIP1, in agreement with our previous observations of STIP1 having a greater binding affinity than the individual domains alone, supporting the notion of multiple binding sites. DP1, the N-terminal PrP-binding domain of STIP1, had no discernible effect on AβO binding with full-length PrP, which agrees with C-terminal PrP being the primary AβO binding site. While DP1 may not actively disrupt AβO interaction with PrP, it may contribute to the greater binding affinity of full length STIP1 binding to PrP and thus its efficacy as an AβO inhibitor. Further investigation will be needed to determine the molecular basis by which DP1, TPR1, and TPR2A domains inhibit PrP-AβO binding in the full-length context.

AβO binding to neurons leads to cell death and impaired synaptic plasticity through multiple signaling pathways [10, 44, 45]. Activation of aberrant NMDAR signaling by AβO to PrP^C resulting in hyper excitability and activation of Fyn kinase has been implicated in dendritic spine loss and neuronal cell death. We found that treatment of primary mouse hippocampal neurons with STIP1, TPR1 or TPR2A reduced the amount of AβO bound to the neuronal surface. Importantly, decrease in AβO binding translated to rescue of neuronal cell death. Consistent with the inability of DP1 to inhibit AβO binding *in vitro*, DP1 had no notable effect on binding of AβO to neurons or on cell death. These results suggest that the TPR1 and TPR2A domains of STIP1 may cooperate for the neuroprotective effects of STIP1 against AβO insult through PrP^C.

Tetratricopeptide repeat motifs are highly degenerate 34 amino acids sequences arranged into helix-loop helix structures forming adjacent anti-parallel helices [46]. The high structural similarity between the TPR1 and TPR2A domains and their similar properties in inhibition of AβO to PrP led us to investigate whether these two regions bind similarly to PrP at the structural level using NMR. Intriguingly, the binding interfaces of TPR1 and TPR2A with PrP differ significantly. PrP bound TPR1 in a short region encompassing the C-terminus of helix 6 and its respective interconnecting loop region with helix 7. This region is far removed from the traditional TPR binding site involved in protein-protein interactions.

The TPR2A interface extends diagonally across a hydrophobic cradle-shaped groove on a single face of the TPR2A molecule [30]. Notably, this region overlaps with the Hsp90 binding site of TPR2A, which is formed by electrostatic interactions with highly conserved carboxylate clamp residues of TPR2A and the C-terminal EEVD motif of Hsp90 [30]. Significant chemical shift changes were observed in residues corresponding to the carboxylate clamp, as well as in additional residues occupying the cradle-shaped groove that binds Hsp90.

While Hsp90 plays an important role in assisting and maintaining the proper folding of many non-natively structured proteins, it has been implicated as detrimental in the clearance of hyper-phosphorylated tau and Aβ, the pathological species in AD [47-49]. Along with this, Hsp90 inhibitors have been shown to be effective in facilitating tau clearance and inhibiting Aβ neurotoxicity in mice [50]. In addition, actively secreted Hsp90 also contributes to the regulation of extracellular client proteins [24, 51]. Given that both STIP1 and Hsp90 are secreted, it is plausible that extracellular Hsp90 may influence STIP1 interaction with PrP in the extracellular matrix or on the cell membrane. Interestingly, while the TPR2A interfaces for Hsp90 and PrP binding show large overlapping regions, PrP binding to STIP1 appears to promote ternary complex formation with Hsp90. PrP binding to STIP1 has been suggested to induce conformational changes in PrP resulting in loss of helical structure [36]. The STIP1 induced unfolding may reveal previously buried hydrophobic pockets on PrP, thus mimicking a misfolded protein and resulting in the recruitment of Hsp90. Alternatively, Hsp90 binding to TPR2A domain of STIP1 may induce structural rearrangements in both proteins, which may hinder STIP1 signaling through PrP. However; the relationship and potential interplay between STIP1, Hsp90 and the PrP is poorly understood and will require further study regarding their roles in the extracellular environment and implications in AD.

STIP1 has traditionally been considered as a cochaperone in the regulation of Hsp70 and Hsp90 client protein folding, however; strong evidence has revealed its importance as a signaling molecule through PrP in neuroprotection [27, 29-31, 35, 52, 53]. The modular structure of STIP1 allows for multiple domains to contribute to complex formation with PrP, which have a direct influence on its protective role against AβO insult. In addition, our studies indicate the possibility of ternary complex

formation composed of PrP, STIP1 and Hsp90, which may influence STIP1 neuroprotective signaling against AβO toxicity in AD.

Author Contribution

Andrzej Maciejewski preformed the experiments and analyzed the data. Valeriy G. Ostapchenko and Flavio H. Beraldo, Vania F. Prado, Marco A. M. Prado, and Wing-Yiu Choy assisted in experimental design and discussion of results. Andrzej Maciejewski, Marco A. M. Prado, and Wing-Yiu Choy wrote the manuscript.

Funding

This work was supported by Canadian Institutes of Health Research (CIHR) (Operating Grants MOP 136930, 126000, 89919); PrioNet-Canada and the Natural Sciences and Engineering Research Council (NSERC) (Discovery Grant RGPIN 06372-2014).

Acknowledgments

We thank the Biomolecular NMR Facility and Bimolecular Interaction and Conformation Facility for their assistance and use of equipment. We would like to thank Anne Brickenden for her technical expertise and discussion.

FIGURE LEGENDS

Figure 1. NMR reveals AβO associate with PrP residues 90-110. (A) ^{1}H-^{15}N HSQC spectra of PrP^{C}(90-231) in the absence (black) and presence (red) of mature $A\beta_{1-42}$ oligomers at a 1:1 ratio. Residues that demonstrate a change in intensity (*black arrows*) or chemical shift changes (*blue arrows*) are noted. (B) Sample of one-dimensional traces of peak intensity presented in (A). Residues 90-231 show a loss in signal intensity (Q91) while C-terminal residues remain unchanged (E221). (C) Normalized peak intensity of PrP (90-231) plotted against residue number. *(black line)* Normalized peak intensity level expected if no interaction took place between PrP (90-231) and $A\beta_{1-42}$ oligomers. *(red line)* Average normalized intensity decrease for all residues of PrP (90-231). (D) Normalized peak intensity of N-terminal PrP (23-95) peaks resolved in the ^{1}H-^{15}N HSQC spectra in the presence of AβO. Due to signal overlap and sequence redundancy, the identity of the residues represented by each peak could not be determined and the thus were assigned an arbitrary number. *(black line)* Normalized peak intensity level expected if no interaction took place between PrP (23-95) and $A\beta_{1-42}$ oligomers. *(red line)* Average normalized intensity decrease for all peaks of PrP (23-95).

Figure 2. DP1, TPR1 and TPR2A associate with PrP^{C}. (A) Domain structure of STIP1 illustrating domain boundaries of three TPR (TPR1, TPR2A and TPR2B) and two DP (DP1 and DP2) domains. (B) Polystyrene plates were pre-coated with 10 μg of PrP (23-231). Wells were probed with various concentrations of STIP1 (B) or STIP1 domains (C). STIP1 or domain immunoreactivity was detected using polyclonal anti-STIP1 antibodies and binding is presented as OD_{495} values. (D) N-terminal PrP (23-95) was incubated with increasing concentrations of STIP1 domains. Binding of the domains was detected as in (B and C) (*n*=3). (E) Immobilized PrP (23-231) was incubated with 1 μM fluorescein-labeled TPR1 in the presence of various concentrations of TPR2A (*n*=4). Fluorescence of bound TPR1 was measured at excitation and emission wavelengths of 485/535 nm, respectively.

Figure 3. TPR1 and TPR2A, but not DP1, inhibit AβO binding to PrP(23-231) *in vitro*. PrP (23-231) was covalently immobilized on to a CM5 sensor chip. (A) Sensograms were collected for various

AβO concentrations binding to PrP (23-231). (B-E) Binding of AβO (2 μM) in the presence of increasing concentrations of STIP1 (B), TPR1 (C), TPR2A (D) or DP1 (E).

Figure 4. STIP1, TPR1 and TPR2A inhibit AβO binding and toxicity in primary mouse hippocampal neurons. (A) Representative images of 13 DIV neurons stained for γ-tubulin (red) and β-amyloid (green) after treatment with AβO in the presence of STIP1, TPR1, TPR2A or DP1. (B) Quantification of A. (C) Comparison of neuronal cell death after 48 hours treatment with AβO (1 μM) alone or in the presence of STIP1 (1 μM), TPR1 (2 μM), TPR2A (2 μM) or DP1 (2 μM). Experiments were analyzed by one-way ANOVA, followed by Tukey's *post hoc* test. ***$P < 0.001$, (n=3).

Figure 5. NMR indicates distinct regions of TPR1 and TPR2A interact with PrP(23-231). (A) Graphical representations of chemical shift changes observed in ^{1}H-^{15}N spectra of ^{15}N-labelled TPR1 or (C) TPR2A in the presence of PrP(23-231). (B) Combined chemical shift changes mapped on to the crystal structure of TPR1 (PDB:1ELW) or (D) TPR2A (PDB:1ELR). The protein structure images are generated using the Chimera molecular graphics software [54].

Figure 6. Hsp90 inhibits STIP1 rescue of primary mouse hippocampal neurons against AβO induced cell death. (A) Chemical shift changes of PrP binding site on TPR2A (top) compared to the solved crystal structure of Hsp90 C-terminal MEEVD peptide bound to TPR2A (bottom) (PDB:1ELR). Residues of TPR2A involved in electrostatic interactions, hydrogen bonding or Van der Waals interactions with Hsp90 peptide are labeled (black). The protein structure images are generated using the Chimera molecular graphics software [54]. (B) Polystyrene plates pre-coated with 10 μg of STI1P were first incubated with increasing concentration of PrP, followed by incubation with Hsp90 (2 μM). Bound Hsp90 was detected using polyclonal anti-Hsp90 antibodies. Binding is presented as OD_{495} values (n=3). (C) Polystyrene plates were pre-coated with 10 μg of full-length PrP (23-231). Wells were probed with various concentrations of Hsp90, followed by detection of bound Hsp90 using polyclonal anti-Hsp90 antibodies. Binding is presented as OD_{495} values (n=3). (D) Comparison of cell death of 13 d neurons after 48 hour treatment with AβO (1 μM) and various concentrations of STIP1 (0-600 nM) in the presence (red) or absence of HSP90 (2 μM) (black) (n=7). Experiments in the

presence or absence of Hsp90 were analyzed by two-way ANOVA, followed by Bonferroni's *post hoc* test. $^{**}P<0.01$.

REFERENCES

1 Cleary, J. P., Walsh, D. M., Hofmeister, J. J., Shankar, G. M., Kuskowski, M. A., Selkoe, D. J. and Ashe, K. H. (2005) Natural oligomers of the amyloid-beta protein specifically disrupt cognitive function. Nat Neurosci. **8**, 79-84

2 Mucke, L. and Selkoe, D. J. (2012) Neurotoxicity of amyloid beta-protein: synaptic and network dysfunction. Cold Spring Harb Perspect Med. **2**, a006338

3 Lambert, M. P., Barlow, A. K., Chromy, B. A., Edwards, C., Freed, R., Liosatos, M., Morgan, T. E., Rozovsky, I., Trommer, B., Viola, K. L., Wals, P., Zhang, C., Finch, C. E., Krafft, G. A. and Klein, W. L. (1998) Diffusible, nonfibrillar ligands derived from Abeta1-42 are potent central nervous system neurotoxins. Proc Natl Acad Sci U S A. **95**, 6448-6453

4 Walsh, D. M., Klyubin, I., Fadeeva, J. V., Cullen, W. K., Anwyl, R., Wolfe, M. S., Rowan, M. J. and Selkoe, D. J. (2002) Naturally secreted oligomers of amyloid beta protein potently inhibit hippocampal long-term potentiation in vivo. Nature. **416**, 535-539

5 Takuma, K., Fang, F., Zhang, W., Yan, S., Fukuzaki, E., Du, H., Sosunov, A., McKhann, G., Funatsu, Y., Nakamichi, N., Nagai, T., Mizoguchi, H., Ibi, D., Hori, O., Ogawa, S., Stern, D. M., Yamada, K. and Yan, S. S. (2009) RAGE-mediated signaling contributes to intraneuronal transport of amyloid-beta and neuronal dysfunction. Proc Natl Acad Sci U S A. **106**, 20021-20026

6 Lauren, J., Gimbel, D. A., Nygaard, H. B., Gilbert, J. W. and Strittmatter, S. M. (2009) Cellular prion protein mediates impairment of synaptic plasticity by amyloid-beta oligomers. Nature. **457**, 1128-1132

7 Freir, D. B., Nicoll, A. J., Klyubin, I., Panico, S., Mc Donald, J. M., Risse, E., Asante, E. A., Farrow, M. A., Sessions, R. B., Saibil, H. R., Clarke, A. R., Rowan, M. J., Walsh, D. M. and Collinge, J. (2011) Interaction between prion protein and toxic amyloid beta assemblies can be therapeutically targeted at multiple sites. Nat Commun. **2**, 336

8 Calella, A. M., Farinelli, M., Nuvolone, M., Mirante, O., Moos, R., Falsig, J., Mansuy, I. M. and Aguzzi, A. (2010) Prion protein and Abeta-related synaptic toxicity impairment. EMBO Mol Med. **2**, 306-314

9 Linden, R., Martins, V. R., Prado, M. A., Cammarota, M., Izquierdo, I. and Brentani, R. R. (2008) Physiology of the prion protein. Physiol Rev. **88**, 673-728

10 Um, J. W., Kaufman, A. C., Kostylev, M., Heiss, J. K., Stagi, M., Takahashi, H., Kerrisk, M. E., Vortmeyer, A., Wisniewski, T., Koleske, A. J., Gunther, E. C., Nygaard, H. B. and Strittmatter, S. M. (2013) Metabotropic glutamate receptor 5 is a coreceptor for Alzheimer abeta oligomer bound to cellular prion protein. Neuron. **79**, 887-902

11 Venkitaramani, D. V., Chin, J., Netzer, W. J., Gouras, G. K., Lesne, S., Malinow, R. and Lombroso, P. J. (2007) Beta-amyloid modulation of synaptic transmission and plasticity. J Neurosci. **27**, 11832-11837

12 Rammes, G., Hasenjager, A., Sroka-Saidi, K., Deussing, J. M. and Parsons, C. G. (2011) Therapeutic significance of NR2B-containing NMDA receptors and mGluR5 metabotropic glutamate receptors in mediating the synaptotoxic effects of beta-amyloid oligomers on long-term potentiation (LTP) in murine hippocampal slices. Neuropharmacology. **60**, 982-990

13 Chen, S., Yadav, S. P. and Surewicz, W. K. (2010) Interaction between human prion protein and amyloid-beta (Abeta) oligomers: role OF N-terminal residues. J Biol Chem. **285**, 26377-26383

14 Younan, N. D., Sarell, C. J., Davies, P., Brown, D. R. and Viles, J. H. (2013) The cellular prion protein traps Alzheimer's Abeta in an oligomeric form and disassembles amyloid fibers. FASEB J. **27**, 1847-1858

15 Gimbel, D. A., Nygaard, H. B., Coffey, E. E., Gunther, E. C., Lauren, J., Gimbel, Z. A. and Strittmatter, S. M. (2010) Memory impairment in transgenic Alzheimer mice requires cellular prion protein. J Neurosci. **30**, 6367-6374
16 Chung, E., Ji, Y., Sun, Y., Kascsak, R. J., Kascsak, R. B., Mehta, P. D., Strittmatter, S. M. and Wisniewski, T. (2010) Anti-PrPC monoclonal antibody infusion as a novel treatment for cognitive deficits in an Alzheimer's disease model mouse. BMC Neurosci. **11**, 130
17 Barry, A. E., Klyubin, I., Mc Donald, J. M., Mably, A. J., Farrell, M. A., Scott, M., Walsh, D. M. and Rowan, M. J. (2011) Alzheimer's disease brain-derived amyloid-beta-mediated inhibition of LTP in vivo is prevented by immunotargeting cellular prion protein. J Neurosci. **31**, 7259-7263
18 Haas, L. T., Kostylev, M. A. and Strittmatter, S. M. (2014) Therapeutic molecules and endogenous ligands regulate the interaction between brain cellular prion protein (PrPC) and metabotropic glutamate receptor 5 (mGluR5). J Biol Chem. **289**, 28460-28477
19 Ostapchenko, V. G., Beraldo, F. H., Mohammad, A. H., Xie, Y. F., Hirata, P. H., Magalhaes, A. C., Lamour, G., Li, H., Maciejewski, A., Belrose, J. C., Teixeira, B. L., Fahnestock, M., Ferreira, S. T., Cashman, N. R., Hajj, G. N., Jackson, M. F., Choy, W. Y., MacDonald, J. F., Martins, V. R., Prado, V. F. and Prado, M. A. (2013) The prion protein ligand, stress-inducible phosphoprotein 1, regulates amyloid-beta oligomer toxicity. J Neurosci. **33**, 16552-16564
20 Brehme, M., Voisine, C., Rolland, T., Wachi, S., Soper, J. H., Zhu, Y., Orton, K., Villella, A., Garza, D., Vidal, M., Ge, H. and Morimoto, R. I. (2014) A chaperome subnetwork safeguards proteostasis in aging and neurodegenerative disease. Cell Rep. **9**, 1135-1150
21 Chen, S. and Smith, D. F. (1998) Hop as an adaptor in the heat shock protein 70 (Hsp70) and hsp90 chaperone machinery. J Biol Chem. **273**, 35194-35200
22 Hajj, G. N., Arantes, C. P., Dias, M. V., Roffe, M., Costa-Silva, B., Lopes, M. H., Porto-Carreiro, I., Rabachini, T., Lima, F. R., Beraldo, F. H., Prado, M. A., Linden, R. and Martins, V. R. (2013) The unconventional secretion of stress-inducible protein 1 by a heterogeneous population of extracellular vesicles. Cell Mol Life Sci. **70**, 3211-3227
23 McCready, J., Sims, J. D., Chan, D. and Jay, D. G. (2010) Secretion of extracellular hsp90alpha via exosomes increases cancer cell motility: a role for plasminogen activation. BMC Cancer. **10**, 294
24 Li, W., Sahu, D. and Tsen, F. (2011) Secreted heat shock protein-90 (Hsp90) in wound healing and cancer. Biochim Biophys Acta. **1823**, 730-741
25 Hegmans, J. P., Bard, M. P., Hemmes, A., Luider, T. M., Kleijmeer, M. J., Prins, J. B., Zitvogel, L., Burgers, S. A., Hoogsteden, H. C. and Lambrecht, B. N. (2004) Proteomic analysis of exosomes secreted by human mesothelioma cells. Am J Pathol. **164**, 1807-1815
26 Zanata, S. M., Lopes, M. H., Mercadante, A. F., Hajj, G. N., Chiarini, L. B., Nomizo, R., Freitas, A. R., Cabral, A. L., Lee, K. S., Juliano, M. A., de Oliveira, E., Jachieri, S. G., Burlingame, A., Huang, L., Linden, R., Brentani, R. R. and Martins, V. R. (2002) Stress-inducible protein 1 is a cell surface ligand for cellular prion that triggers neuroprotection. EMBO J. **21**, 3307-3316
27 Caetano, F. A., Lopes, M. H., Hajj, G. N., Machado, C. F., Pinto Arantes, C., Magalhaes, A. C., Vieira Mde, P., Americo, T. A., Massensini, A. R., Priola, S. A., Vorberg, I., Gomez, M. V., Linden, R., Prado, V. F., Martins, V. R. and Prado, M. A. (2008) Endocytosis of prion protein is required for ERK1/2 signaling induced by stress-inducible protein 1. J Neurosci. **28**, 6691-6702
28 Lopes, M. H., Hajj, G. N., Muras, A. G., Mancini, G. L., Castro, R. M., Ribeiro, K. C., Brentani, R. R., Linden, R. and Martins, V. R. (2005) Interaction of cellular prion and stress-inducible protein 1 promotes neuritogenesis and neuroprotection by distinct signaling pathways. J Neurosci. **25**, 11330-11339

29 Beraldo, F. H., Arantes, C. P., Santos, T. G., Queiroz, N. G., Young, K., Rylett, R. J., Markus, R. P., Prado, M. A. and Martins, V. R. (2010) Role of alpha7 nicotinic acetylcholine receptor in calcium signaling induced by prion protein interaction with stress-inducible protein 1. J Biol Chem. **285**, 36542-36550
30 Scheufler, C., Brinker, A., Bourenkov, G., Pegoraro, S., Moroder, L., Bartunik, H., Hartl, F. U. and Moarefi, I. (2000) Structure of TPR domain-peptide complexes: critical elements in the assembly of the Hsp70-Hsp90 multichaperone machine. Cell. **101**, 199-210
31 Onuoha, S. C., Coulstock, E. T., Grossmann, J. G. and Jackson, S. E. (2008) Structural studies on the co-chaperone Hop and its complexes with Hsp90. J Mol Biol. **379**, 732-744
32 Lee, C. T., Graf, C., Mayer, F. J., Richter, S. M. and Mayer, M. P. (2012) Dynamics of the regulation of Hsp90 by the co-chaperone Sti1. EMBO J. **31**, 1518-1528
33 Rohl, A., Wengler, D., Madl, T., Lagleder, S., Tippel, F., Herrmann, M., Hendrix, J., Richter, K., Hack, G., Schmid, A. B., Kessler, H., Lamb, D. C. and Buchner, J. (2015) Hsp90 regulates the dynamics of its cochaperone Sti1 and the transfer of Hsp70 between modules. Nat Commun. **6**, 6655
34 Southworth, D. R. and Agard, D. A. (2011) Client-loading conformation of the Hsp90 molecular chaperone revealed in the cryo-EM structure of the human Hsp90:Hop complex. Mol Cell. **42**, 771-781
35 Schmid, A. B., Lagleder, S., Grawert, M. A., Rohl, A., Hagn, F., Wandinger, S. K., Cox, M. B., Demmer, O., Richter, K., Groll, M., Kessler, H. and Buchner, J. (2012) The architecture of functional modules in the Hsp90 co-chaperone Sti1/Hop. EMBO J. **31**, 1506-1517
36 Romano, S. A., Cordeiro, Y., Lima, L. M., Lopes, M. H., Silva, J. L., Foguel, D. and Linden, R. (2009) Reciprocal remodeling upon binding of the prion protein to its signaling partner hop/STI1. FASEB J. **23**, 4308-4316
37 Maciejewski, A., Prado, M. A. and Choy, W. Y. (2012) (1)H, (1)(5)N and (1)(3)C backbone resonance assignments of the TPR1 and TPR2A domains of mouse STI1. Biomol NMR Assign. **7**, 305-310
38 Delaglio, F., Grzesiek, S., Vuister, G. W., Zhu, G., Pfeifer, J. and Bax, A. (1995) NMRPipe: a multidimensional spectral processing system based on UNIX pipes. J Biomol NMR. **6**, 277-293
39 Johnson, B. A. and Blevins, R. A. (1994) NMR View: A computer program for the visualization and analysis of NMR data. J Biomol NMR. **4**, 603-614
40 Hornemann, S., von Schroetter, C., Damberger, F. F. and Wuthrich, K. (2009) Prion protein-detergent micelle interactions studied by NMR in solution. J Biol Chem. **284**, 22713-22721
41 Lacor, P. N., Buniel, M. C., Furlow, P. W., Clemente, A. S., Velasco, P. T., Wood, M., Viola, K. L. and Klein, W. L. (2007) Abeta oligomer-induced aberrations in synapse composition, shape, and density provide a molecular basis for loss of connectivity in Alzheimer's disease. J Neurosci. **27**, 796-807
42 Fluharty, B. R., Biasini, E., Stravalaci, M., Sclip, A., Diomede, L., Balducci, C., La Vitola, P., Messa, M., Colombo, L., Forloni, G., Borsello, T., Gobbi, M. and Harris, D. A. (2013) An N-terminal fragment of the prion protein binds to amyloid-beta oligomers and inhibits their neurotoxicity in vivo. J Biol Chem. **288**, 7857-7866
43 Balducci, C., Beeg, M., Stravalaci, M., Bastone, A., Sclip, A., Biasini, E., Tapella, L., Colombo, L., Manzoni, C., Borsello, T., Chiesa, R., Gobbi, M., Salmona, M. and Forloni, G. (2010) Synthetic amyloid-beta oligomers impair long-term memory independently of cellular prion protein. Proc Natl Acad Sci U S A. **107**, 2295-2300
44 Um, J. W. and Strittmatter, S. M. (2012) Amyloid-beta induced signaling by cellular prion protein and Fyn kinase in Alzheimer disease. Prion. **7**, 37-41

45 Khan, G. M., Tong, M., Jhun, M., Arora, K. and Nichols, R. A. (2010) beta-Amyloid activates presynaptic alpha7 nicotinic acetylcholine receptors reconstituted into a model nerve cell system: involvement of lipid rafts. Eur J Neurosci. **31**, 788-796
46 Cortajarena, A. L. and Regan, L. (2006) Ligand binding by TPR domains. Protein Sci. **15**, 1193-1198
47 Blair, L. J., Nordhues, B. A., Hill, S. E., Scaglione, K. M., O'Leary, J. C., 3rd, Fontaine, S. N., Breydo, L., Zhang, B., Li, P., Wang, L., Cotman, C., Paulson, H. L., Muschol, M., Uversky, V. N., Klengel, T., Binder, E. B., Kayed, R., Golde, T. E., Berchtold, N. and Dickey, C. A. (2013) Accelerated neurodegeneration through chaperone-mediated oligomerization of tau. J Clin Invest. **123**, 4158-4169
48 Ansar, S., Burlison, J. A., Hadden, M. K., Yu, X. M., Desino, K. E., Bean, J., Neckers, L., Audus, K. L., Michaelis, M. L. and Blagg, B. S. (2007) A non-toxic Hsp90 inhibitor protects neurons from Abeta-induced toxicity. Bioorg Med Chem Lett. **17**, 1984-1990
49 Dickey, C. A., Kamal, A., Lundgren, K., Klosak, N., Bailey, R. M., Dunmore, J., Ash, P., Shoraka, S., Zlatkovic, J., Eckman, C. B., Patterson, C., Dickson, D. W., Nahman, N. S., Jr., Hutton, M., Burrows, F. and Petrucelli, L. (2007) The high-affinity HSP90-CHIP complex recognizes and selectively degrades phosphorylated tau client proteins. J Clin Invest. **117**, 648-658
50 Luo, W., Dou, F., Rodina, A., Chip, S., Kim, J., Zhao, Q., Moulick, K., Aguirre, J., Wu, N., Greengard, P. and Chiosis, G. (2007) Roles of heat-shock protein 90 in maintaining and facilitating the neurodegenerative phenotype in tauopathies. Proc Natl Acad Sci U S A. **104**, 9511-9516
51 Liao, D. F., Jin, Z. G., Baas, A. S., Daum, G., Gygi, S. P., Aebersold, R. and Berk, B. C. (2000) Purification and identification of secreted oxidative stress-induced factors from vascular smooth muscle cells. J Biol Chem. **275**, 189-196
52 Coitinho, A. S., Lopes, M. H., Hajj, G. N., Rossato, J. I., Freitas, A. R., Castro, C. C., Cammarota, M., Brentani, R. R., Izquierdo, I. and Martins, V. R. (2007) Short-term memory formation and long-term memory consolidation are enhanced by cellular prion association to stress-inducible protein 1. Neurobiol Dis. **26**, 282-290
53 Roffe, M., Beraldo, F. H., Bester, R., Nunziante, M., Bach, C., Mancini, G., Gilch, S., Vorberg, I., Castilho, B. A., Martins, V. R. and Hajj, G. N. (2010) Prion protein interaction with stress-inducible protein 1 enhances neuronal protein synthesis via mTOR. Proc Natl Acad Sci U S A. **107**, 13147-13152
54 Pettersen, E. F., Goddard, T. D., Hung, C. C., Couch, G. S., Greenblatt, D. M., Meng, E. C., Ferrin, T. E. (2004) J Comput Chem **25**, 1605-1612.

A

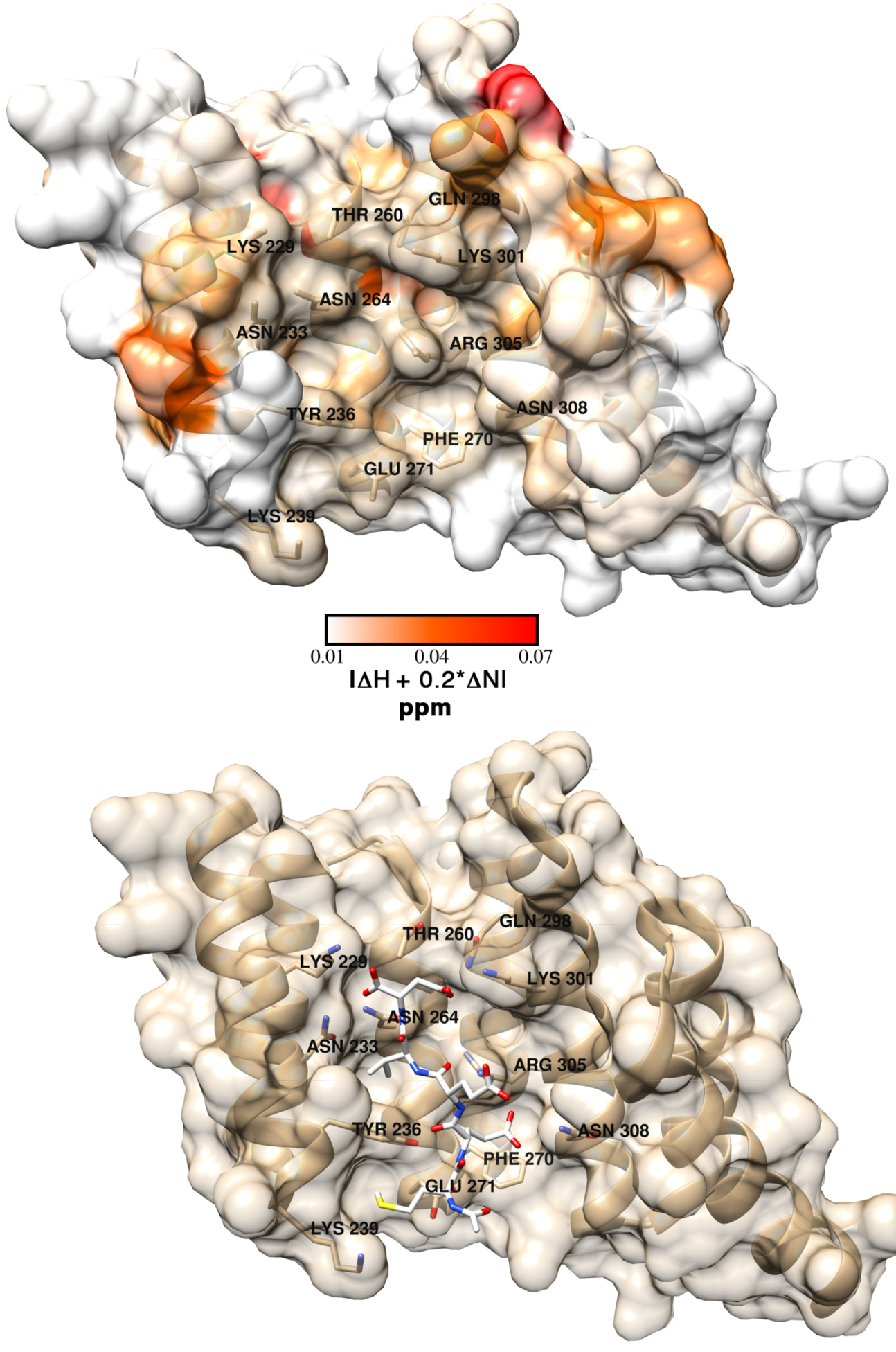
GLN 298
THR 260
LYS 229
LYS 301
ASN 264
ASN 233
ARG 305
TYR 236
ASN 308
PHE 270
GLU 271
LYS 239
0.01
0.04
0.07
IΔH + 0.2*ΔNI
ppm
GLN 298
THR 260
LYS 229
LYS 301
ASN 264
ASN 233
ARG 305
TYR 236
ASN 308
PHE 270
GLU 271
LYS 239

B

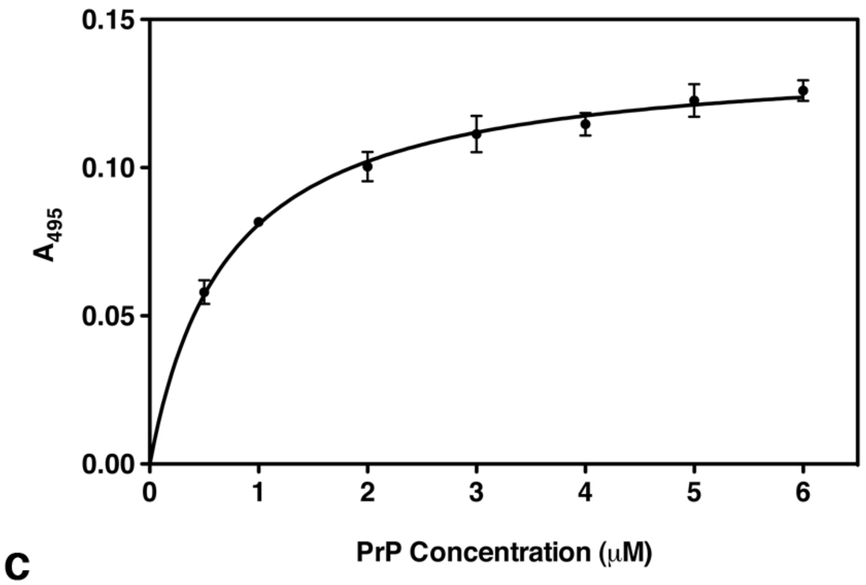
0.15
0.10
0.05
0.00
A495
0
1
2
3
4
5
6
PrP Concentration (μM)

C

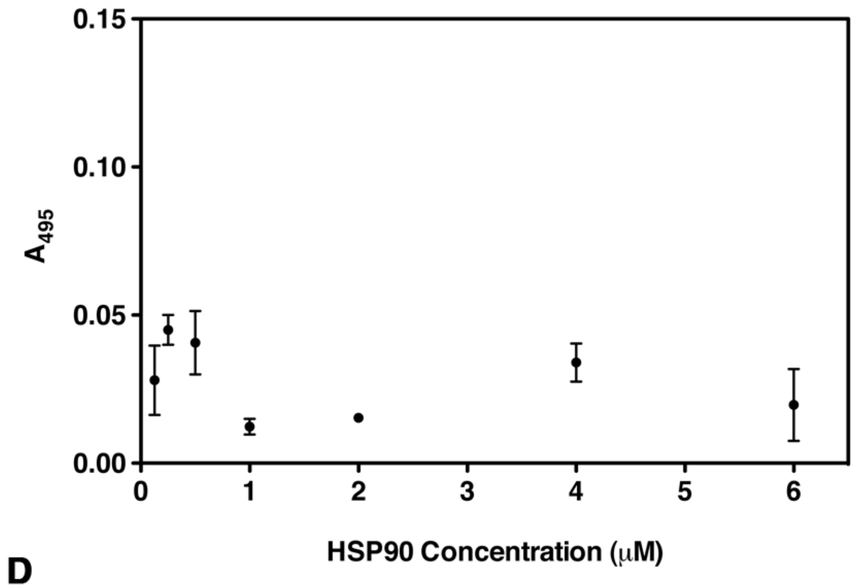
0.15
0.10
0.05
0.00
A495
0
1
2
3
4
5
6
HSP90 Concentration (μM)

D

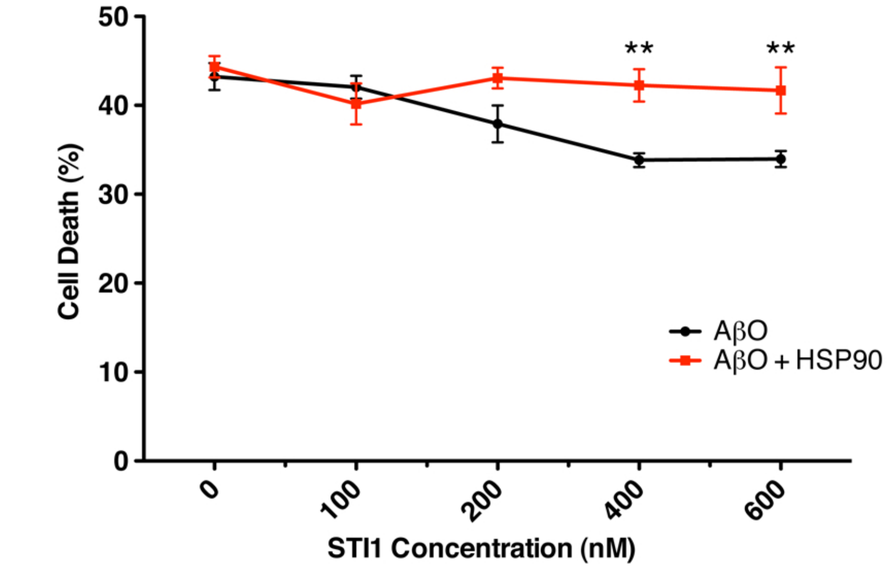
50
40
30
20
10
0
Cell Death (%)
**
**
AβO
AβO + HSP90
0
100
200
400
600
STI1 Concentration (nM)

A

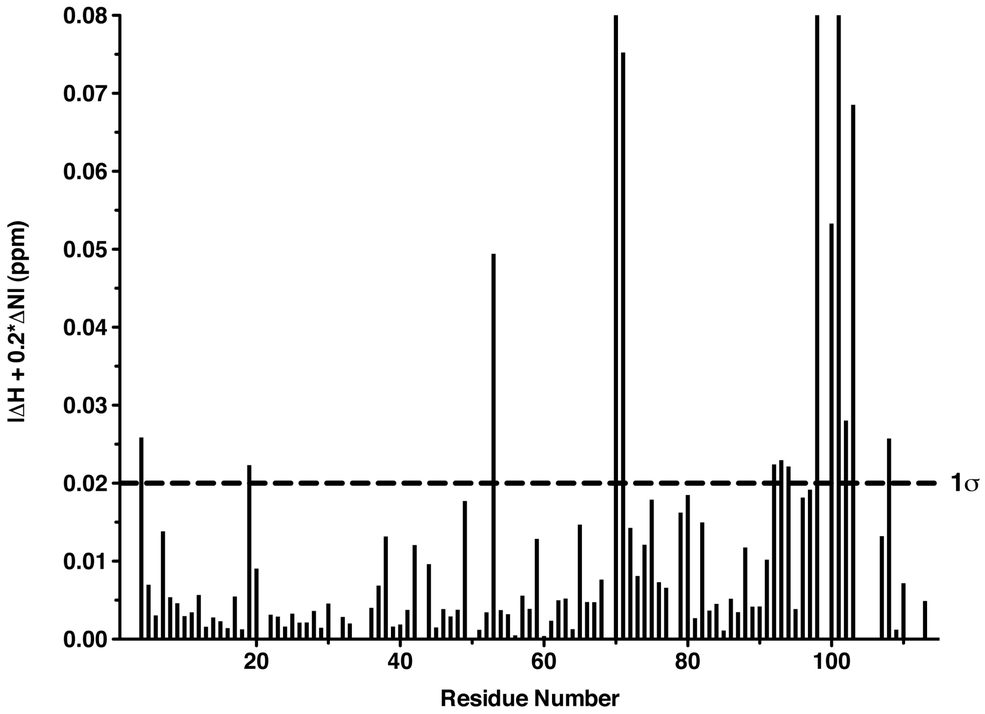
0.08
0.07
0.06
0.05
0.04
0.03
0.02
0.01
0.00
|ΔH + 0.2*ΔNl (ppm)
1σ
20
40
60
80
100
Residue Number

B

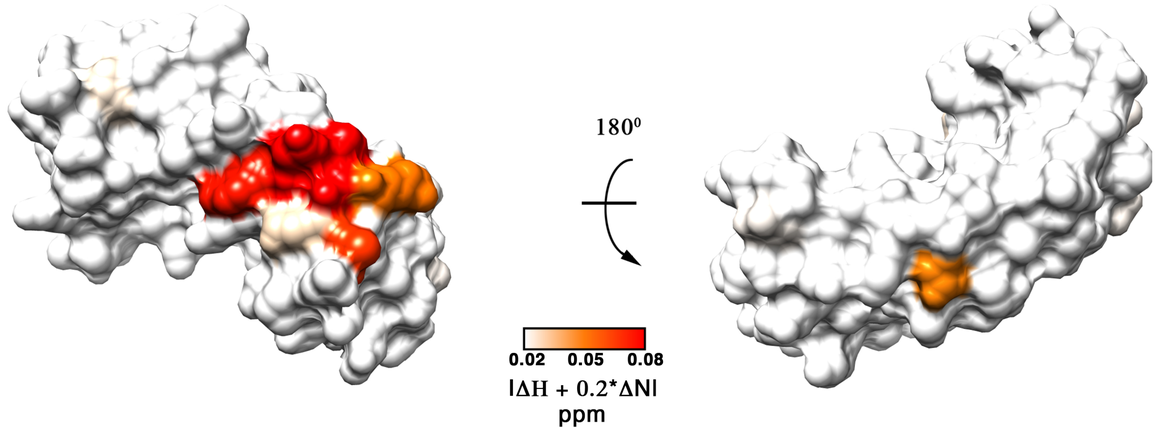
180⁰
0.02 0.05 0.08
|ΔH + 0.2*ΔNl
ppm

C

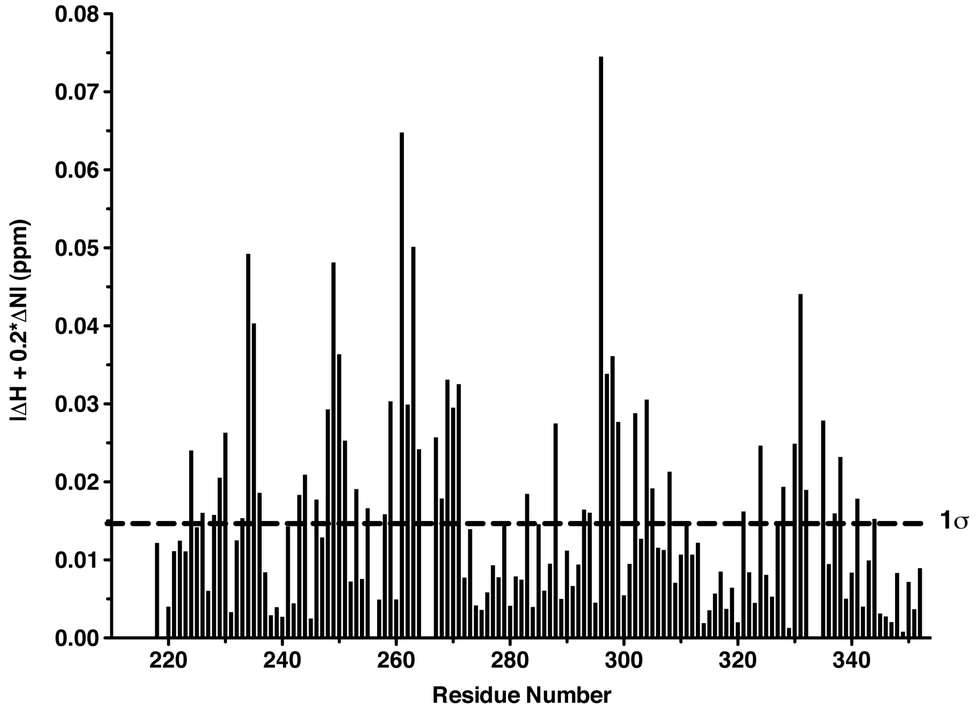
0.08
0.07
0.06
0.05
0.04
0.03
0.02
0.01
0.00
|ΔH + 0.2*ΔNl (ppm)
1σ
220
240
260
280
300
320
340
Residue Number

D

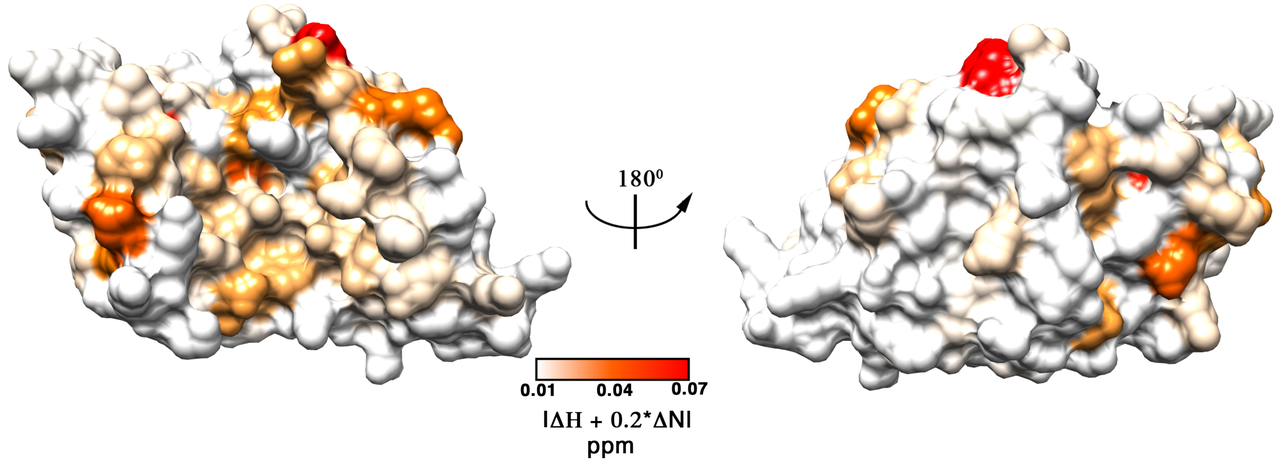
180⁰
0.01 0.04 0.07
|ΔH + 0.2*ΔNl
ppm

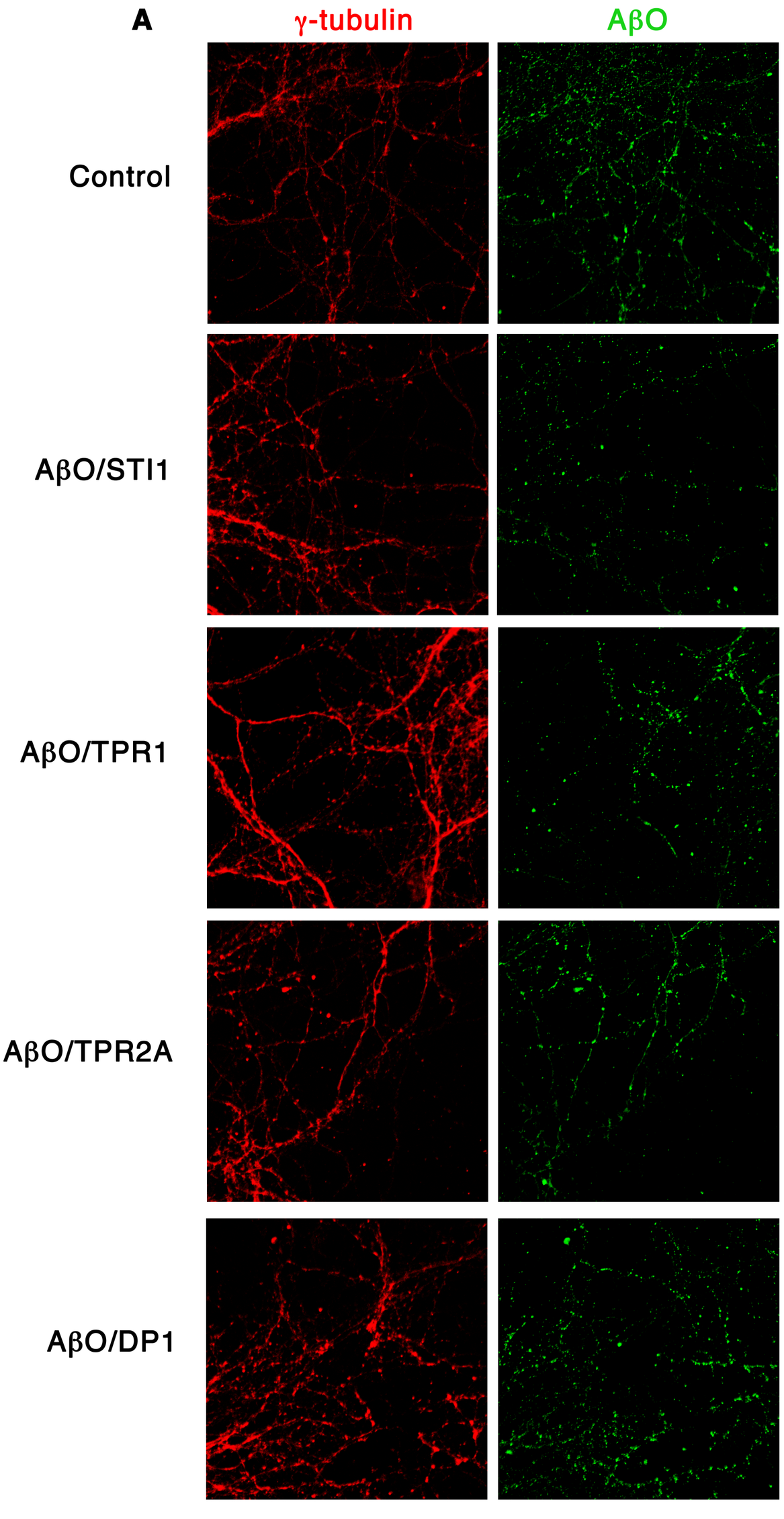
A
γ-tubulin
AβO
Control
AβO/STI1
AβO/TPR1
AβO/TPR2A
AβO/DP1

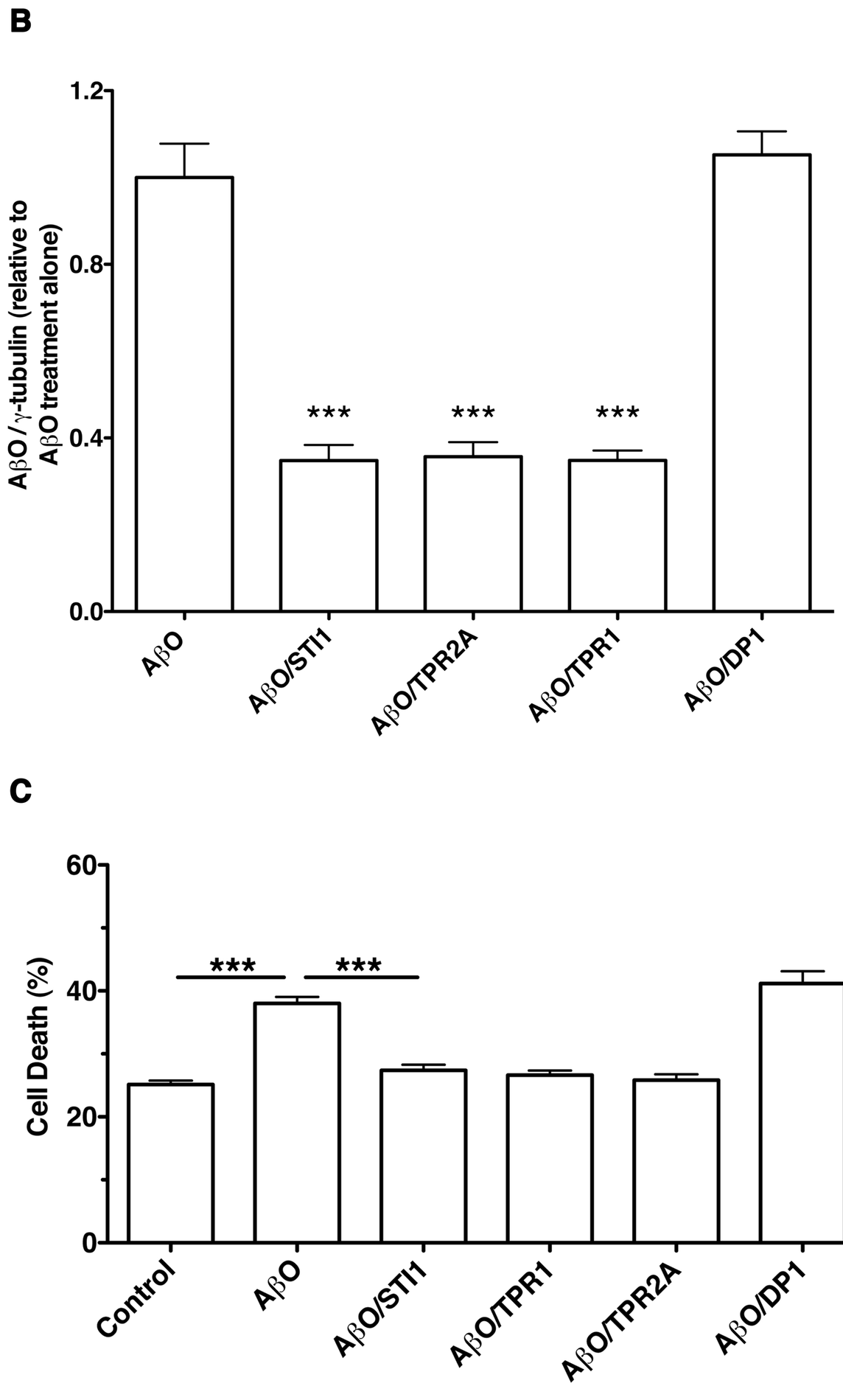
B
AβO/γ-tubulin (relative to AβO treatment alone)
1.2
0.8
0.4
0.0
***
***
***
AβO
AβO/STI1
AβO/TPR2A
AβO/TPR1
AβO/DP1

C
Cell Death (%)
60
40
20
0
***
***
Control
AβO
AβO/STI1
AβO/TPR1
AβO/TPR2A
AβO/DP1

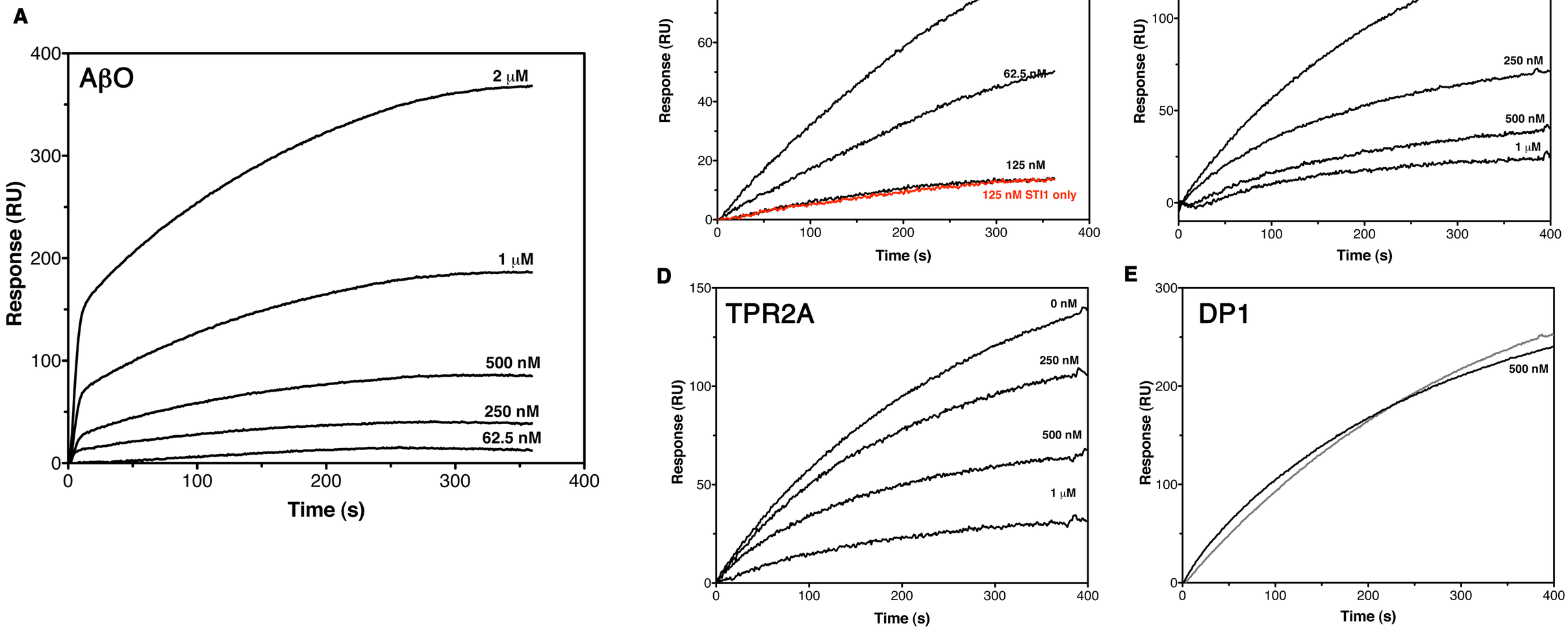
A
AβO
2 μM
1 μM
500 nM
250 nM
62.5 nM
Response (RU)
Time (s)
B
STIP1
0 nM
62.5 nM
125 nM
125 nM STI1 only
Response (RU)
Time (s)
C
TPR1
0 nM
250 nM
500 nM
1 μM
Response (RU)
Time (s)
D
TPR2A
0 nM
250 nM
500 nM
1 μM
Response (RU)
Time (s)
E
DP1
500 nM
Response (RU)
Time (s)

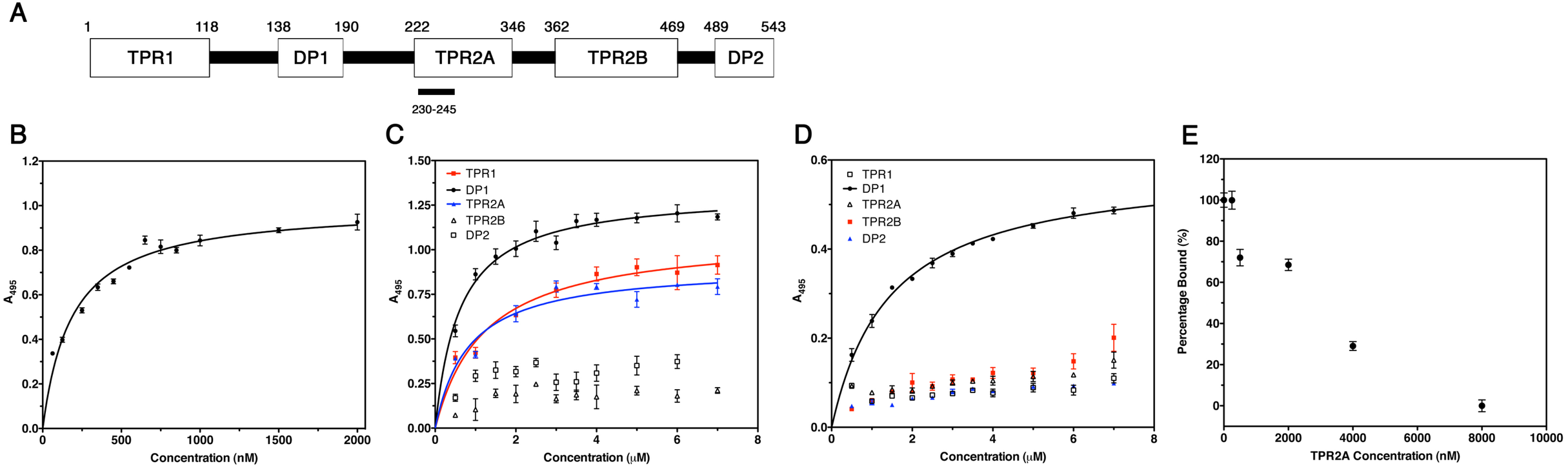
A
1
118
138
190
222
346
362
469
489
543
TPR1
DP1
TPR2A
TPR2B
DP2
230-245
B
A495
Concentration (nM)
C
TPR1
DP1
TPR2A
TPR2B
DP2
A495
Concentration (μM)
D
TPR1
DP1
TPR2A
TPR2B
DP2
A495
Concentration (μM)
E
Percentage Bound (%)
TPR2A Concentration (nM)

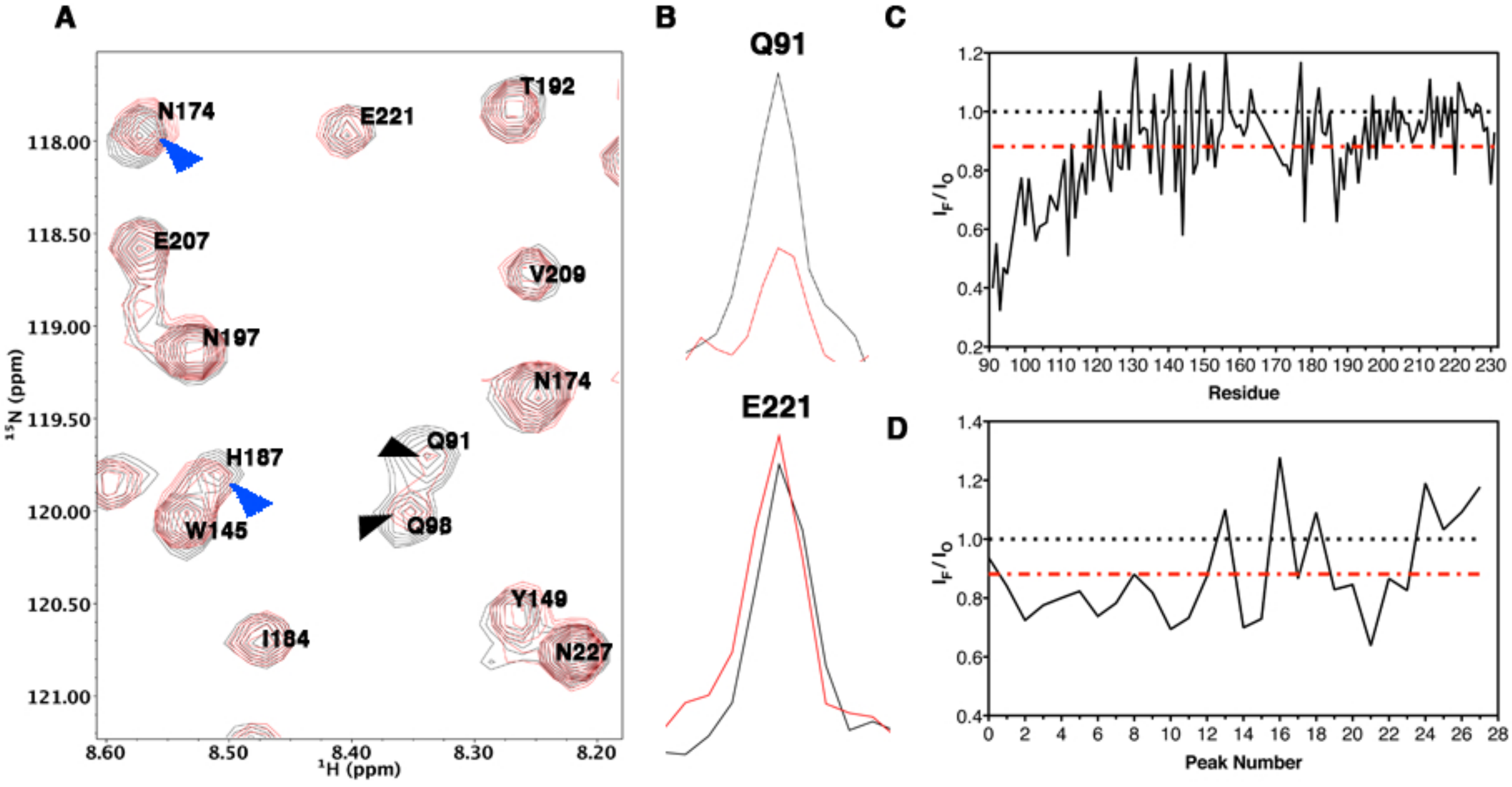
A
N174
E221
T192
E207
V209
N197
N174
Q91
H187
W145
Q98
Y149
I184
N227
118.00
118.50
119.00
119.50
120.00
120.50
121.00
^{15}N (ppm)
8.60
8.50
8.40
8.30
8.20
^{1}H (ppm)
B
Q91
E221
C
1.2
1.0
0.8
0.6
0.4
0.2
I_F / I_O
90 100 110 120 130 140 150 160 170 180 190 200 210 220 230
Residue
D
1.4
1.2
1.0
0.8
0.6
0.4
I_F / I_O
0 2 4 6 8 10 12 14 16 18 20 22 24 26 28
Peak Number